Impact of Post-Oxidation Annealing on Low-Frequency Noise, Threshold Voltage, and Subthreshold Swing of p-Channel MOSFETs

A. K. M. Ahsan, *Student Member, IEEE* and D. K. Schroder, *Life Fellow, IEEE*

***Abstract*—The impact of post-oxidation annealing on the low-frequency noise, threshold voltage, and subthreshold swing of p-channel MOSFET is reported. The low-frequency noise is improved significantly with post-oxidation annealing and a modest V_T and *S* reduction is observed. Oxide traps are primarily extracted from measured noise. They are also extracted from threshold voltage and subthreshold slope shift. The contribution of oxide traps to threshold voltage shift and $1/f$ noise is analyzed through quantitative approach in the light of correlated fluctuation theory. Analysis on experimental results shed light on the well-known controversy about the origin of low-frequency noise, suggesting that experimental results are in agreement with mobility fluctuation theory whereas correlated number fluctuation theory explains the result assuming only a fraction of total oxide charge at a given energy level participates in the generation of low-frequency noise.**

***Index Terms*—Interface-trap density, low-frequency noise, oxide-trap density, post-oxidation annealing, scattering parameter, silicon, silicon dioxide, subthreshold swing, threshold voltage.**

I. INTRODUCTION

HIGH-TEMPERATURE oxides yield better oxides and silicon–oxide interfaces than those grown at low temperatures [1]–[3]. As the technology is scaled to thinner gate oxides, the oxidation temperature, and oxidation rate are periodically reduced for better oxide thickness control [4], [5]. Post-oxidation annealing ensures better oxide and interface quality. An improvement of oxide quality was observed through low-frequency noise data after post-oxidation annealing. This anneal also affects the device threshold voltage, V_T, and subthreshold swing, *S*. In this letter, we extract the change of oxide-trap density and interface-trap density after annealing through low-frequency noise [6] and current–voltage (*I–V*) measurements of p-channel MOSFETs. We separate the contribution of interface trap charge from the contribution of oxide charge and show the effect on V_T, S, and low-frequency noise. We also discussed the experimental result to shed light on the well-known controversy about the origin of low-frequency noise [7].

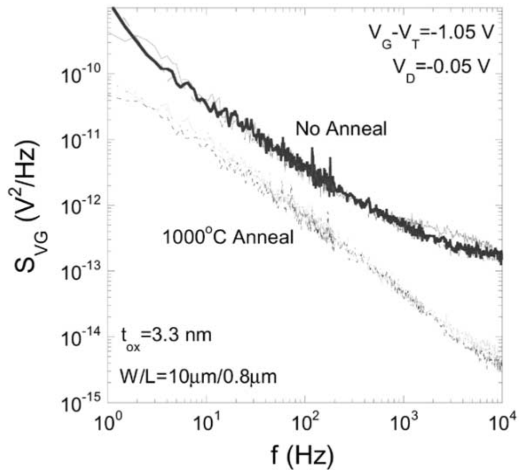

Fig. 1. Gate voltage noise spectrum density for a p-channel MOSFET. Three sets of measured noise data are shown $|V_G–V_T| = 1.05$ V.

II. DEVICE TECHNOLOGY AND MEASUREMENT

The p-channel MOSFETs with gate area 10×0.8 μm^2 were fabricated in a standard CMOS process on (100)-oriented Si substrates with gate oxide (oxynitride) thickness of 3.3 nm. The threshold voltage after appropriate ion implantation was -0.45 V. Boron-doped p$^+$ poly-silicon gates were used with a thickness of 160 nm. Boron diffusion into oxide is controlled by minimizing the thermal exposure after depositing the poly and oxynitride is less susceptible to boron diffusion. We have assumed in our analysis that the boron penetration into the oxide is minimized and it does not play significant passivating action with interface. The wafers were annealed at 1000 °C for 15 min immediately following the gate oxide growth.

An automatic noise measurement system (BTA 9812A) was used for detection and amplification of the noise current generated by the device under test (DUT). A semiconductor parameter analyzer (HP4142B) and a dynamic signal analyzer (HP35665A) were used to measure *I–V* characteristics and noise spectrum, respectively.

III. RESULTS AND DISCUSSION

Low-frequency noise measurements were made on devices from three wafers fabricated under identical process conditions to include the wafer-to-wafer variation. Fig. 1 shows the input referred noise spectrum density, S_{VG}, versus frequency at a gate overdrive voltage of $|V_G–V_T| = 1.05$ V. It is obvious from the figure that the noise level improves significantly after annealing.

Manuscript received January 5, 2004. This work was supported in part by the National Science Foundation (NSF) State/Industry/University Cooperative Research Centers' Center for Low Power Electronics (CLPE) under Grant #EEC-9 523 338. The review of this letter was arranged by Editor E. Sangiorgi.

The authors are with the Department of Electrical Engineering, Arizona State University, Tempe, AZ 85287-5706 USA.

Digital Object Identifier 10.1109/LED.2004.825170

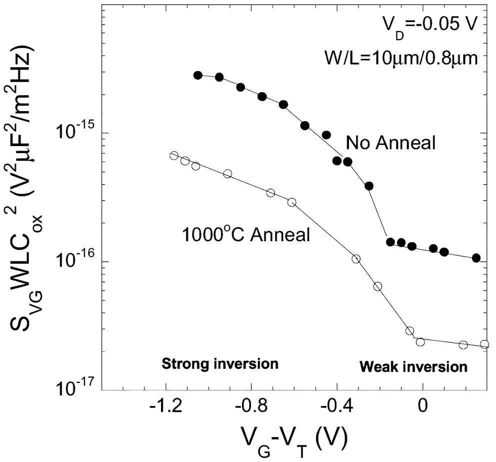

Fig. 2. Normalized gate voltage noise spectrum density versus gate overdrive voltage. The noise is extracted at frequency 100 Hz at low drain voltage ($V_D = -50$ mV).

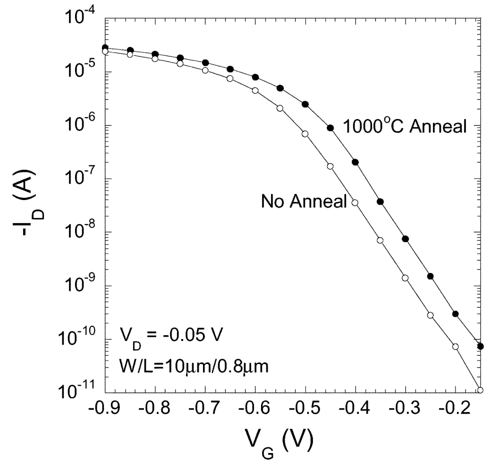

Fig. 3. Drain current versus gate voltage with and without post-oxidation annealing. The threshold voltage reduction is $|\Delta V_T| = 52$ mV.

Fig. 2 shows the normalized gate voltage noise spectrum density, $S_{\rm VG}{\rm WLC}_{\rm ox}^2$, at $f = 100$ Hz for different gate overdrive voltages. The *I–V* characteristics in Fig. 3 show a V_T shift of 52 mV and a small improvement in the subthreshold swing from 71.4 to 70.4 mV/dec.

The measurements show the input referred noise spectrum density to increase from weak inversion to strong inversion. It is almost constant in the weak inversion region, consistent with the unified $1/f$ noise model [8], [9]. According to this model, the gate voltage noise spectrum density is

$$S_{\rm VG}(f) = \frac{kTq^2}{\alpha WLC_{\rm ox}^2 f}(1+\sigma\mu_{\rm eff}N_s)^2 N_{\rm ot} \tag{1}$$

where α is the attenuation coefficient, $\mu_{\rm eff}$ the effective carrier mobility, σ the Coulombic scattering parameter, N_s the number of channel carriers/unit area, $C_{\rm ox}$ the gate oxide capacitance/unit area, *WL* the gate area, and $N_{\rm ot}$ the oxide-trap density (cm^{-3} eV^{-1}).

The oxide-trap and interface trap densities are extracted from the low-frequency noise, the threshold voltage shift, and the subthreshold slope change. Using the unified noise model, $N_{\rm ot} = 5 \times 10^{16}$ cm^{-3} eV^{-1} for the annealed oxide, extracted from the measured noise data in weak inversion in Fig. 2. This is significantly lower than that of the unannealed device (2.5×10^{17} cm^{-3}eV^{-1}), leading to the changing trap density of 2×10^{17} cm^{-3}eV^{-1}. The value for the unannealed device is very similar to the values of 2–5 $\times 10^{17}$ cm^{-3}eV^{-1} in [10] and [11]. From the extracted trap density, the Coulombic scattering parameter σ is found to be 7×10^{-15} Vs, very close to the published values of 4–8 $\times 10^{-15}$ Vs [8], [11].

The threshold voltage change as a result of changing oxide charge and interface trap densities, can be expressed as [12]

$$\Delta V_T = \frac{\Delta Q_{\rm ox} + \Delta Q_{\rm it}(\phi_s)}{C_{\rm ox}} = \frac{\Delta Q}{C_{\rm ox}} \tag{2}$$

where $\Delta Q{\rm it}$ is the interface trap charge density change, and $\Delta Q{\rm ox}$ the oxide charge density change. $Q{\rm ox}$ is usually positive, and that portion of $Q{\rm it}$ that contributes to the threshold voltage in p-channel MOSFETs is also positive, being due to donor states between the surface potential and the Fermi energy. From the V_T alone, we can only determine the total charge change $\Delta{\rm Q}$, not the individual components. The observed 52-mV positive V_T shift with anneal is consistent with a reduction of total charge, leading to $\Delta Q/q = 3.4 \times 10^{11}$ cm^{-2}.

The subthreshold swing change is $\Delta S = ({\rm kT}/q)\ln 10(\Delta Q{\rm it}/C_{\rm ox})$. Hence, combining the V_T shift with the subthreshold swing change allows a separation of $\Delta Q{\rm ox}$ and $\Delta{\rm Q}_{\rm it}$. The change of subthreshold swing of 1 mV/dec due to post-oxidation annealing is extracted from the *I–V* plot in Fig. 3. Assuming this interface-trap density to be constant in the bandgap around the bandgap center, the interface-trap charge change is extracted as $\Delta Q{\rm it}(\phi_{\rm B})/{\rm q} = \Delta{\rm D}_{\rm it}\phi_{\rm B} = 1.08 \times 10^{11}$ cm^{-2}, where $\phi_{\rm B} = ({\rm kT/q})\ln(N_{\rm A}/N_{\rm i}) = 0.43$ V is the Fermi potential. From (2), we then obtain $\Delta Q{\rm ox}/{\rm q} = 2.32 \times 10^{11}$ cm^{-2}.

What do these various charges/traps represent? Is there any correlation between the $N_{\rm ot}$ extracted from the $1/f$ noise measurement, and the $Q{\rm ox}$ and ${\rm D}_{\rm it}$ extracted from the V_T and S shift (*I–V* measurement)? The $N_{\rm ot}$ that produce $1/f$ noise, are those around the Fermi level at a given gate voltage. Within the context of correlated noise theory, the trap density, $N_{\rm ot}$ does not vary much with energy [10]. So it is justified to assume that $N_{\rm ot}$ is almost constant over the energy. Assuming the Fermi-level sweeps an energy of about $\phi_{\rm B}$ between weak and strong inversion, the change in trap density becomes $\Delta N_{\rm ot}\phi_{\rm B} = 8.6 \times 10^{16}$ cm^{-3}. Further, assuming these charges to be uniformly distributed through the oxide gives a per-unit area density of 2.8×10^{10} cm^{-2}. This is lower than the $\Delta Q{\rm ox}/{\rm q} = 2.32\times10^{11}$ cm^{-2} extracted from the V_T shift. From these values, we speculate that only a fraction of the total charge at a given energy level in the oxide participates in the low-frequency noise. Most of the oxide charge does not exchange charge with channel carriers.

The above approach of explaining experimental results relies on the unified $1/f$ noise theory, which combines number fluctuation and correlated mobility fluctuation and suffers from objection [13] that it cannot predict $1/f$ noise accurately for p-type MOSFETs. On the other hand, the pure mobility fluctuation theory [14]–[16] uses an empirical relationship where the relative $1/f$ noise is inversely proportional to the number

TABLE I
α_H PARAMETER CALCULATED FROM EXPERIMENTAL RESULTS PRESENTED IN FIGS. 1 AND 2

Bias	No Anneal	Anneal	Equation used for calculation
Linear region	1.8×10^{-4}	3.7×10^{-5}	$S_{VG}=\alpha_H q(V_G-V_T)/WLC_{OX}f$ [7]
Subthreshold region	1.2×10^{-4}	3.1×10^{-5}	$S_{VG}=\alpha_H \eta^2 kT/WLC_{OX}f$ [17] With $\eta^2 \sim 2$ in $I \sim e^{qVg/\eta kT}$

of carriers and proportional to a parameter α_H [14]–[16]. Our experimental result can be explained successfully by using this approach and the extracted α_H values are summarized in Table I which are reasonable [7], [15].

IV. CONCLUSION

The impact of post-oxidation annealing on low-frequency noise, threshold voltage, and subthreshold swing of p-channel MOSFETs is investigated. A reduction of all three is observed. The different mode of contribution of oxide traps to $1/f$ noise and to threshold voltage are discussed. We find the total charge in the oxide and at the SiO_2/Si interface (from V_T and S data) to be higher than that extracted from $1/f$ noise data using a unified model, which brought the conclusion that either only a fraction of the total oxide charge at a given energy level participates in the generation of low-frequency noise or $1/f$ noise is a mobility fluctuation phenomenon which can be explained by mobility fluctuation models with empirical parameter α_H.

REFERENCES

[1] B. E. Deal and A. S. Grove, "General relationship for the thermal oxidation of silicon," *J. Appl. Phys.*, vol. 36, pp. 3770–3778, Dec. 1965.

[2] Z. Q. Yao, H. B. Harrison, S. Dimitrijev, and Y. T. Yeow, "Effects of nitric oxide annealing of thermally grown silicon dioxide characteristics," *IEEE Electron Device Lett.*, vol. 16, pp. 345–347, Aug. 1995.

[3] E. H. Nicollian and J. R. Brews, *MOS Physics and Technology*. New York: Wiley, 1982.

[4] S. C. Su, "Low temperature silicon processing techniques for VLSI fabrication," *Solid-State Technol.*, vol. 24, pp. 72–82, Mar. 1981.

[5] S. Wolf and R. N. Tauber, *Silicon Processing for the VLSI Era: Process Technology*. Sunset Beach, CA: Lattice, Sept. 1986.

[6] E. Simoen, A. Mercha, and C. Claeys, "Noise diagnostics of advanced silicon substrates and deep submicron process modules," in *Analytical and Diagnostic Techniques for Semiconductor Materials, Devices, and Processes*, B. O. Kolbesen, C. Claeys, P. Stallhofer, F. Tradiff, D. K. Schroder, T. J. Shaffner, M. Tajima, and P. Rai-Choudhury, Eds. Pennington, NJ: Electrochem. Soc., 2003, pp. 420–439.

[7] L. K. J. J Vandamme, X. Li, and D. Rigaud, "$1/f$ noise in MOS devices, mobility or number fluctuations?," *IEEE Trans. Electron Devices*, vol. 41, pp. 1936–1945, Nov. 1994.

[8] K. K. Hung, P. K. Ko, C. Hu, and Y. C. Cheng, "A unified model for flicker noise in metal oxide semiconductor field effect transistors," *IEEE Trans. Electron Devices*, vol. 37, pp. 654–665, Mar. 1990.

[9] ——, "A physics based MOSFET noise model for circuit simulators," *IEEE Trans. Electron Devices*, vol. 37, pp. 1323–133, May 1990.

[10] R. Jayaraman and C. G. Sodini, "A $1/f$ noise technique to extract the oxide-trap density near the conduction band edge of silicon,," *IEEE Trans. Electron Devices*, vol. 36, pp. 1773–1782, Sept. 1989.

[11] M. Fadlallah, G. Ghibaudo, J. Joomah, and G. Guegan, "Static and low frequency noise characterization in surface- and buried-mode 0.1 μm PMOSFETs," *Solid State Electron.*, vol. 47, pp. 1155–1160, July 2003.

[12] D. K. Schroder, *Semiconductor Material and Device Characterization*, 2nd ed. New York: Wiley, 1998.

[13] E. P. Vandamme and L. K. J. Vandamme, "Critical discussions on unified noise models for MOSFETs," *IEEE Trans. Electron Devices*, vol. 47, pp. 2146–2152, Nov. 2000.

[14] R. H. M. Clevers, "Volume and temperature dependence of the $1/f$ noise parameter α in Si," *Phys. B*, vol. 154, pp. 214–224, 1989.

[15] L. K. J. Vandamme and S. Oosterhoff, "Annealing of ion-implanted resistors reduce the $1/f$ noise," *J. Appl. Phys.*, vol. 59, pp. 3169–3174, May 1986.

[16] F. N. Hooge and L. K. J. Vandamme, "Lattice scattering causes $1/f$ noise," *Phys. Lett. A*, vol. 66, pp. 315–316, May 1978.

[17] E. P. Vandamme and L. K. J. Vandamme, "Unsolved problems on $1/f$ noise in MOSFETs and possible solutions," in *Proc. Int. Conf. Unsolved Problem of Noise and Fluctuations*, Adelaide, Australia, 1999, pp. 481–486.